Proceedings of Space Nuclear Conference 2007
Boston, Massachusetts, June 24-28 2007
Paper 2047

High Fidelity Thermal Simulators for Non-Nuclear Testing: Analysis and Initial Results

Shannon M. Bragg-Sitton[1], Ricky Dickens[1], David Dixon[2]
[1]*NASA Marshall Space Flight Center, Nuclear Systems Branch / ER24, MSFC, AL 35812*
[2]*North Carolina State University, Raleigh, NC*
Tel: 256.544.6272, E-Mail: Shannon.M.Bragg-Sitton@nasa.gov

Abstract – *Non-nuclear testing can be a valuable tool in the development of a space nuclear power system, providing system characterization data and allowing one to work through various fabrication, assembly and integration issues without the cost and time associated with a full ground nuclear test. In a non-nuclear test bed, electric heaters are used to simulate the heat from nuclear fuel. Testing with non-optimized heater elements allows one to assess thermal, heat transfer, and stress related attributes of a given system, but fails to demonstrate the dynamic response that would be present in an integrated, fueled reactor system. High fidelity thermal simulators that match both the static and the dynamic fuel pin performance that would be observed in an operating, fueled nuclear reactor can vastly increase the value of non-nuclear test results. With optimized simulators, the integration of thermal hydraulic hardware tests with simulated neutronic response provides a bridge between electrically heated testing and fueled nuclear testing, providing a better assessment of system integration issues, characterization of integrated system response times and response characteristics, and assessment of potential design improvements at a relatively small fiscal investment. Initial conceptual thermal simulator designs are determined by simple one-dimensional analysis at a single axial location and at steady state conditions; feasible concepts are then input into a detailed three-dimensional model for comparison to expected fuel pin performance. Static and dynamic fuel pin performance for a proposed reactor design is determined using SINDA/FLUINT thermal analysis software, and comparison is made between the expected nuclear performance and the performance of conceptual thermal simulator designs. Through a series of iterative analyses, a conceptual high fidelity design can developed. Test results presented in this paper correspond to a "first cut" simulator design for a potential liquid metal (NaK) cooled reactor design that could be applied for Lunar surface power. Proposed refinements to this simulator design are also presented.*

I. INTRODUCTION

At the NASA Marshall Space Flight Center (MSFC) Early Flight Fission Test Facility (EFF-TF) electric heaters are used to simulate the heat from nuclear fuel to test potential space fission power and propulsion systems. To allow early utilization, nuclear system designs must be relatively simple, easy to fabricate, and easy to test using non-nuclear heaters to closely mimic heat from fission. In this test strategy, specialized electric heaters are used to simulate the heat from nuclear fuel, allowing one to develop an understanding of individual components and integrated system operation without the cost, time and safety concerns associated with nuclear testing. Electric heaters have been used for this purpose in numerous terrestrial and space reactor test and development programs.[1-5] The thermal simulators (heaters) developed at the EFF-TF have been applied in a variety of space reactor concepts for power or propulsion applications, including heat pipe, direct gas, and liquid metal cooled reactor systems.[6-9] To accurately represent the fuel, the simulators should be capable of matching the overall properties of the nuclear fuel elements rather than simply matching the fuel element temperatures during nominal operation. In addition to matching the total core power and core power profile (axial and radial), this includes matching thermal stresses in the pin, effective radial pin conductivities, and transient pin characteristics (affected by the effective radial pin density and heat capacity) during both static and dynamic test conditions.

Thermal simulators previously designed and tested at the EFF-TF were constructed to meet the individual pin power levels and to roughly emulate the axial power distribution of specific reactor designs.[10,11] The current design effort focuses on developing thermal simulators that are fully instrumented and that mimic the transient nuclear fuel pin performance under typical transient operations.

II. DESIGN PROCESS

A rigorous simulator design process begins with the definition of the nuclear reactor design and characterization of the nuclear fuel pin performance. Given this information, the simulator design can commence with iterative conceptual design. Comparison of fuel pin and simulator performance is made at the outer surface of the fuel pin clad and the thermal simulator sheath, assessing the temperature variation at the clad or sheath surface as a function of axial position during steady state operation at nominal pin power levels and as a function of time during prescribed transient operations (e.g. ±25% power, ±25% coolant mass flow rate, and full shutdown).

The EFF-TF is currently working toward the potential development of an affordable fission surface power (FSP) system that could be deployed on the Lunar surface. Through a strong partnership with engineers at the Los Alamos National Laboratory (LANL), conceptual reactor designs are translated into hardware for non-nuclear testing at NASA MSFC. A liquid metal cooled reactor was selected for further reactor design and test activities. This design was derived from the only fission system that the United States has deployed for space operation, the Systems for Nuclear Auxiliary Power (SNAP) 10a reactor, which was launched in 1965.[12] This "best estimate" reactor design was selected in early 2006 to allow hardware development tests to proceed. Development of test hardware and test techniques for a "best estimate" design allows engineers at MSFC to assess the feasibility of select design features and to work through fabrication issues associated with potential future hardware development.

Simulators developed prior to the current effort did not include instrumentation within the simulator itself; instead, core temperatures were discerned using thermocouples (TCs) inserted into open regions of the core where possible (e.g. heat pipe cooled reactor), mounted to the outer core vessel or inserted in the coolant flow (gas cooled and initial liquid metal cooled systems). One of the primary goals of the simulator development at MSFC is to develop simulators that can be fully instrumented to directly measure the axial pin temperatures throughout the system operation. A full core array might include ~100-500 pins; while only a fraction of these pins would be instrumented, careful placement of instrumented simulator elements that takes advantage of core symmetry will allow full characterization of the axial and radial core temperatures. A few select positions should also be instrumented to ensure that off-nominal performance (e.g. skewed power profiles) can be detected.

II.A. Baseline Reactor Design

Current simulator development is based on a potential Fission Surface Power Primary Test Circuit (FSP-PTC) reactor design. This design is a derivative of the SNAP reactor designs[12] and could be deployed on the Lunar surface. The design basis will be referred to as the SNAPf3 concept. The SNAPf3 is a thermal spectrum reactor designed to operate at 98 kWt (25 kWe) with reactor cooling provided by pumped liquid metal (sodium potassium, NaK-78) at inlet and outlet temperatures of 840 K and 880 K, respectively. The SNAPf3 incorporates 114 UZrH fuel pins, yielding an average pin power of 0.86 kW thermal (kWt); the peak-to-average power ratio of 1.24, calculated with the neutron transport code MCNPX, yields a maximum pin power of 1.07 kWt. The overall core assembly is constructed from stainless steel 316 (SS316).

II.B. Initial Simulator Design

Prior to receiving detailed requirements regarding the desired thermal simulator performance under static and transient conditions for the SNAPf3 concept (the first step in a thorough iterative design process), a design and fabrication feasibility study was initiated to allow hardware work to progress. The primary objective of this exercise was to scope out potentially feasible design concepts and to work through any potential manufacturing issues given the geometry and total power requirements for a SNAPf3 fuel pin. Note that the main difference between this and the primary, high fidelity simulator design development is that the nuclear design is used only to produce a rough conceptual design for the simulator without completing the detailed performance optimization that seeks to achieve transient performance matching. This "initial" simulator design is then used as a starting point for the iterative, high fidelity conceptual design while answering various hardware feasibility questions.

Design criteria established for the initial simulator design require that the simulator:

1. Meet the geometric and power requirements of the baseline reactor design;
2. Accommodate testing of various axial power profiles without full disassembly;
3. Incorporate imbedded instrumentation; and
4. Minimize simulator disturbance of the coolant flow plenum.

In order to match the pin thermal stresses and to adhere to the core material composition where possible, SS316 was selected for the simulator sheath (corresponding to the fuel

pin clad material). Additionally, simulator geometric dimensions (length and outer sheath diameter) were selected to correspond to that of the fuel pin clad.

The primary purpose in designing for heater swap-out (requirement 2) is to allow testing of various power profiles within the same overall core configuration without requiring that NaK be flushed from the system. Additionally, it is anticipated that the simulator sheaths will be welded to the full core vessel to ensure reliable seals, such that it will not be possible to swap out the full simulator assembly (including sheath and imbedded TCs) even if the liquid metal is flushed from the core.

The current design allows 13 TCs (or fiber optics) to be installed in the simulator: 6 TCs on the sheath outer diameter (OD), 6 TCs on the sheath inner diameter (ID) and one TC at the centerline of the heater element. TCs are used for initial simulator tests in a high purity helium environment and with a water-cooled calorimeter; later testing in a NaK flow cell, which emulates the NaK flow path around a single simulator, will incorporate 3 fiber optics on the ID of the sheath to provide additional temperature distribution data. Fiber optic instrumentation can allow temperature measurement at intervals as small as one centimeter,[13] but they have a delayed time response relative to TCs and, therefore, are not sufficient for real-time feedback control. Control for the NaK flow cell and future core array testing will rely on TC instrumentation.

A simulator design that incorporates a necked down region was pursued in accordance with requirements 2 and 4 above. In the nuclear fueled design, the fuel pins do not penetrate the coolant flow plenum but are instead anchored at a mounting plate at the plenum boundary. However, simulators require penetration through this region to allow power inlet/outlet to the individual pins. Power integration becomes more complex if the reactor design requires a pressure vessel or if the selected coolant is electrically conductive, as in liquid metal cooled systems. Integration is accomplished by extending the simulator sheath through the flow plenum, which can impact the flow dynamics. In attempt to minimize this impact, the sheath OD is reduced as much as possible through the plenum, while still allowing sufficient clearance for electrical connections and heater element removal. The current design reduces the cross sectional area of the simulators in the plenum region to just one sixth of the area that would be taken if the simulator OD was held constant through this region, reducing the impact on the flow distribution within the NaK plenum. Computational fluid dynamics (CFD) analysis is planned to quantify this benefit but has not yet been completed due to limited resource availability. This simulator design concept is shown in Fig. 1.

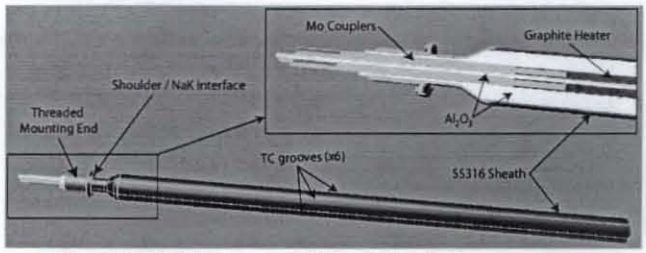

Fig. 1. Initial instrumented simulator design.

A schematic of the nuclear fuel pin and simulator concepts is provided in Fig. 2. The initial thermal simulator design (Fig. 2b) is constructed using a graphite heater element, a solid alumina insulator, and a SS316 sheath. Gaps between the graphite/alumina and alumina/SS316 are filled by high purity helium gas at 100 torr. TC grooves (0.28mm, 0.011") cut into the sheath OD track the sheath contour and exit through small holes cut into the shoulder; these holes are continued through the threaded mounting end and are completely contained within the threads. Matching grooves are cut into the OD of the insulator (0.53mm, 0.021") to allow placement of TCs or fiber optics. An alternate "stage 2" simulator, designed and procured at the same time as the initial design, reduces the OD of the solid alumina and allows the second gas gap to be filled with a material selected to better match the fuel pin performance. Because the engineering design and procurement process can be very extended, design decisions often have to be made very early in the design process to allow fabrication issues to be addressed while the high fidelity design progresses. Lessons learned through the initial simulator design and fabrication are currently being incorporated in high fidelity simulator design.

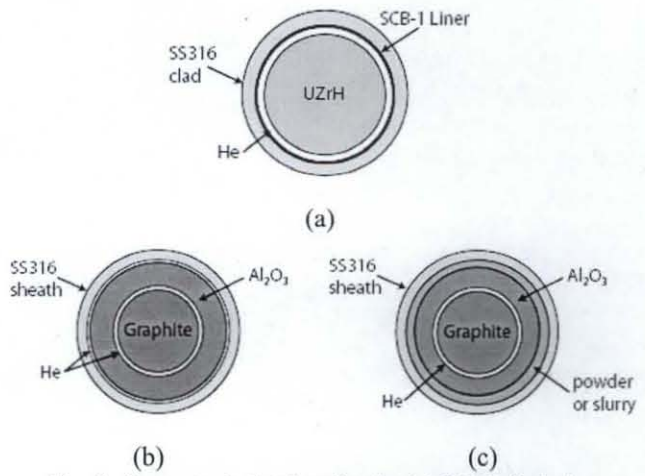

Fig. 2. Conceptual sketches for the (a) UZrH fuel element, (b) initial simulator design and (c) "stage 2" simulator design.

$$T_{\max,FE} = q'\left[\frac{1}{4\pi\bar{k}_f} + \frac{1}{2\pi R_g h_g} + \frac{1}{2\pi R_l \left/ k_l/\delta_l\right.} + \frac{\ln\left(R_{co}/R_{ci}\right)}{2\pi k_c} + \frac{1}{2\pi R_{co} h}\right] + T_{bulk} \quad (1)$$

$$T_{\max,Sim} = q'\left[\frac{1}{4\pi\bar{k}_h} + \frac{1}{2\pi R_{g1} h_{g1}} + \frac{\ln\left(R_{io}/R_{ii}\right)}{2\pi k_i} + \frac{1}{2\pi R_{g2} h_{g2}} + \frac{\ln\left(R_{si}/R_{io}\right)}{2\pi k_x} + \frac{\ln\left(R_{so}/R_{si}\right)}{2\pi k_s} + \frac{1}{2\pi R_{so} h}\right] + T_{bulk} \quad (2)$$

II.C. High Fidelity Simulator Design

After initial simulator designs (Figs. 1, 2) were complete and procurements placed, detailed pin performance criteria were received from LANL reactor designers, allowing the high fidelity simulator design to officially commence. A "first cut" material selection is made based on a simplified one dimensional analysis of pin performance during steady state operation at a selected axial position. Applicable equations are provided in equations (1) and (2).

In equation (1), $T_{max,FE}$ represents the maximum fuel element temperature, and each term represents the temperature rise from the bulk coolant temperature, T_{bulk}, across each subsequent layer of the element. Sequentially, these terms represent the temperature drop (from $T_{max,FE}$) across the fuel, gas gap, clad liner, fuel pin clad, and convective cooling of the clad. Equation (2) provides the maximum simulator temperature, $T_{max,Sim}$, and the individual terms represent the temperature drop across the heater element, first gas gap, insulator layer, second gas gap (Fig. 2b design), slurry material fill (Fig. 2c), sheath, and convective cooling of the sheath. In each case, the given symbols are defined as such: k, thermal conductivity; h, convection coefficient; R_g, average gap radius; R_o, R_i, outer and inner layer radius.

Following 1-D analysis, feasible concepts are input into a detailed three-dimensional model developed using Thermal Desktop (TD).[14] Static and dynamic fuel pin performance is determined using SINDA/FLUINT thermal analysis software (which interfaces with TD),[15] and comparison is made between the expected nuclear performance and the performance of conceptual thermal simulator designs.

For assessment of the initial simulator performance a symmetric simulator is modeled in TD for Sinda/Fluint analysis; no attempt is made to model end effects. Due to the additional mass at either end of the simulator (bottle neck extension and end cap), the model is expected to predict higher than measured temperatures at either end of the simulator. This will be shown in the test and analysis results provided for the initial simulator design (see III.B).

III. CURRENT HARDWARE DEVELOPMENT AND TESTING

The initial instrumented thermal simulator (Fig. 2b design) has been fabricated and assembled and initial testing is currently under way. Theoretical and experimental analysis of potential fill materials to replace the second He gas gap (Fig. 2c design) has also commenced.

III.A. Initial Simulator Assembly

Simulator hardware currently under test is shown in Fig. 3, in which the locations for the sheath and insulator TCs are identified. TCs are run through the TC feed holes on the bottle neck end of the sheath and lie in grooves along the length of the sheath. The openings at the shoulder of the simulator will be brazed closed prior to final assembly and testing in NaK. The tip of each TC is held in position using a 0.005 cm (0.002") thick, 2.5 cm (1") long piece of nickel foil that is tack welded to the sheath surface.

Assembly of the initial instrumented simulator hardware is shown in Fig. 4. In the photos shown, the external TCs have already been installed. The internal TCs are installed by first aligning the TCs in the grooves on the bottle neck section of the insulator; these are held in place temporarily using a small piece of tape that allow the TC wires to move through the groove without slipping out of the groove. Once the bottle neck piece is in place, the straight cylindrical alumina sections can be installed. The measurement end of each TC is secured at the desired location on the alumina cylinders using alumina cement. TCs are located at 1.9, 6.4, 16.5, 26.7, 36.8, and 41.3 cm (0.75, 2.5, 6.5, 10.5, 14.5 and 16.25") on the insulator and sheath, with subsequent TCs in adjacent grooves (30° apart). After all TCs have been installed, the end cap is installed at the non-power end of the simulator. Prior to test, the tape used to aid TC installation is removed and the central graphite heater element is installed and connected to the power supply.

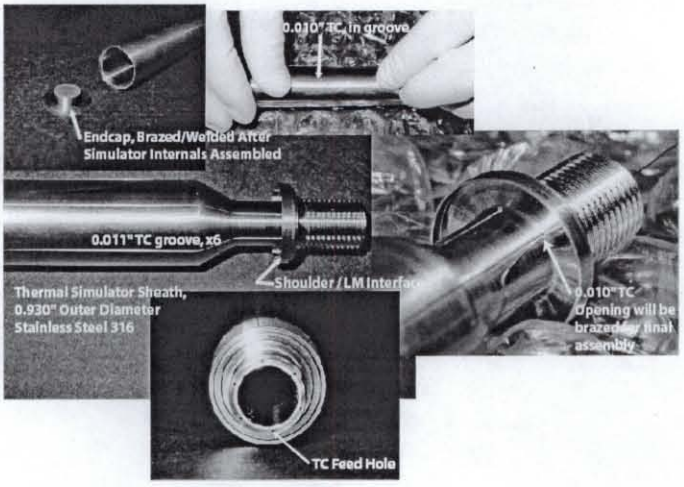

(a)

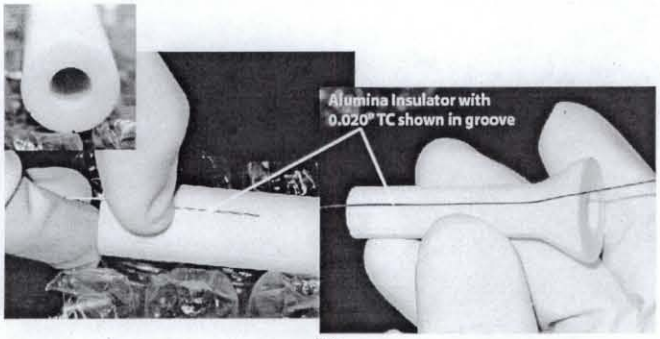

(b)

Fig. 3. Initial instrumented simulator components: (a) stainless steel sheath and (b) alumina insulators.

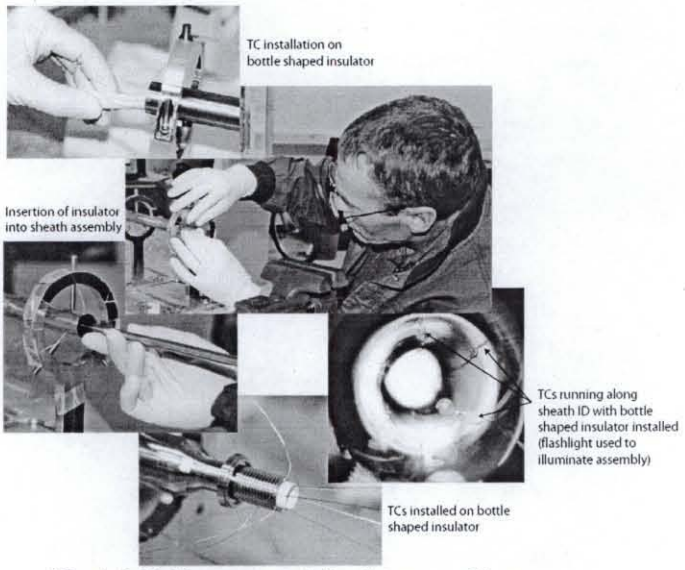

Fig. 4. Initial instrumented simulator assembly process.

III.B. Initial Simulator Tests

To prevent any potential deformation of the simulator sheath due to rapid heating, rapid cooling, or localized heating, the power levels are approached in ramp fashion over 30 minutes to minimize thermal stresses on the pin and the maximum allowed sheath temperature is set to 650°C for tests in which no active cooling is provided to the element. In the actual core environment, the clad temperature is not expected to exceed 615°C (888 K) with the fuel pin operating at 1075 W, as predicted by SINDA/FLUINT. The bare instrumented thermal simulator is tested up to 625 W in a 100 torr helium environment. The maximum tested power level will be increased to the nominal operating levels of 860 and 1075 W (nominal average and peak pin power in the SNAPf3 design) during later tests that incorporate active heat removal using a water cooled calorimeter or a flowing NaK environment, but the same temperature limit will be imposed.

As seen in the comparison of the data presented in Fig. 5, the predicted simulator sheath temperatures suggest a relatively flat and symmetric axial temperature profile. This results from the model representation of the simulator as a purely symmetric geometry with constant diameter; no attempt was made to represent the bottle-shaped end section at the power lead end of the simulator or the end cap at the opposite end. A more accurate, detailed representation of the axial simulator geometry is currently being added to the model to more accurately represent the simulator and to better validate the thermal model.

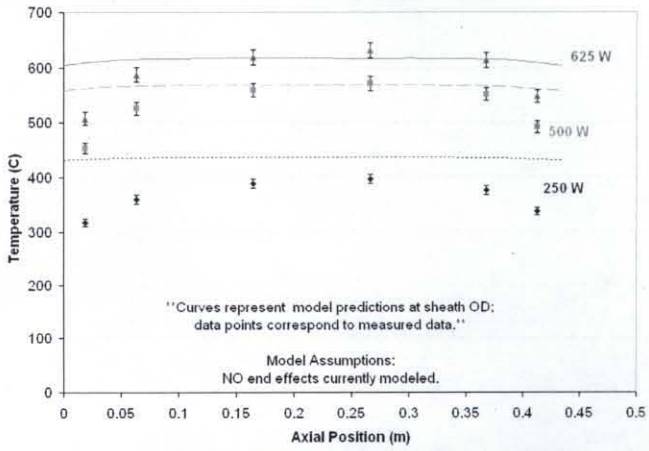

Fig. 5. Analysis and experimental results for steady state testing of the initial instrumented simulator.

Initial transient testing of the thermal simulator has been completed. Two cases were considered: a 25% power increase from steady state operation at 500 W (to 625 W) and a 20% power decrease from steady state operation at 625 W (to 500 W). Results are provided in Fig. 6 for thermocouples located at 16.5 cm (6.5", TC9) and 26.7 cm (10.5", TC10) on the simulator sheath, along with the

predicted simulator response at the axial midpoint from Sinda/Fluint (transient initialized at time zero).

The analysis and experimental data indicate that the simulator temperature returns to the original temperature after a transient (see temperature at 500 W in Fig. 6a,b), demonstrating that the simulator is not permanently modified by operation at increased power and temperature. Transient tests have been repeated on 4 separate test days; representative results are presented in Fig. 6.

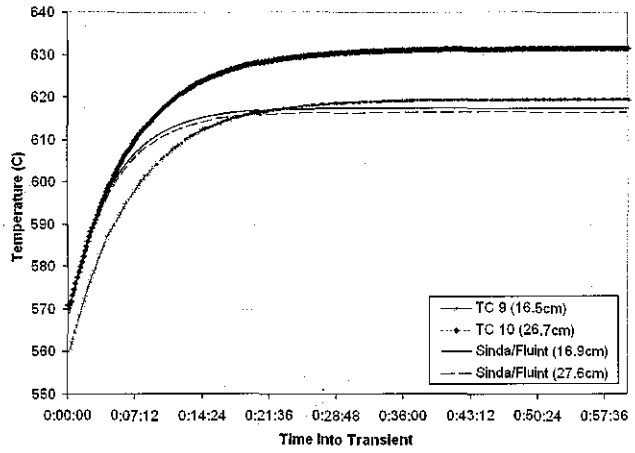

(a)

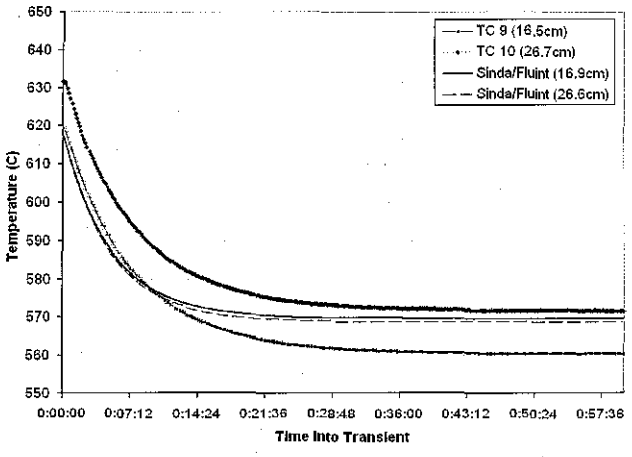

(b)

Fig. 6. Transient thermal analysis and test data for (a) 25% power increase from 500 to 625 W and (b) 20% power decrease from 625 to 500 W.

Thermal analysis predicts slightly more rapid heating/cooling of the element than observed experimentally, suggesting that some of the parameters and material properties used in the model may differ somewhat from the actual configuration. Properties such as thermal conductivity, density and specific heat are taken from the literature, and emissivities (used in radiation calculations across the gas gaps or from the outer sheath surface) are estimated based on literature values and the visible condition of the emitting material. In the experimental data, TCs 9 and 10 are located symmetrically about the axial midpoint of the simulator. However, TC 10 was consistently hotter in the transient data; this is also true of the steady state data, in which the power lead end of the simulator is approximately 40°C cooler at the power inlet end at 625 W and at 500 W; the temperature difference was reduced to ~21°C at 250 W resulting from the lower operating temperature. The asymmetry is likely due to the larger heat sink at the power feed end of the simulator, causing the temperature to be slightly more depressed at that end. Additionally, the power feed end is "open," allowing radiation heat loss from the element in addition to conductive losses (along the sheath and through the power leads), although the view factor from the heater element to the cool chamber wall is relatively small due to the extended bottle shape.

III.C. Fill Material Analysis and Testing

Thermal analysis of a single fuel pin with a flowing NaK boundary condition, having an inlet and outlet NaK temperature of 567 and 607°C (840 and 880 K), respectively, was compared to the predicted performance of a thermal simulator with the same boundary condition. As is evident from the results presented in Fig. 7, the theoretical simulator performance is vastly improved by omitting the second gas gap and replacing the gas with a thermal coupling material, such as powdered alumina.

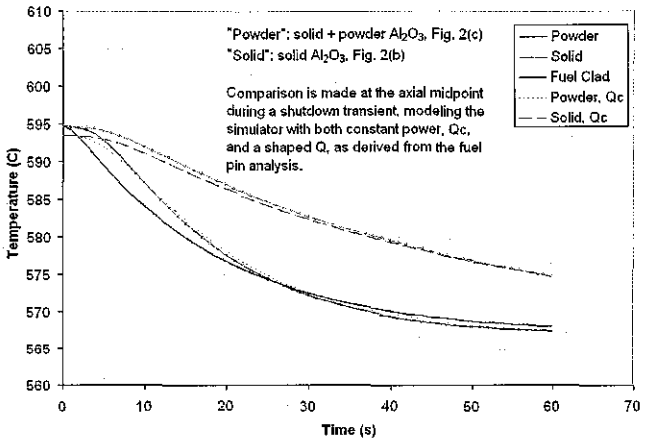

Fig. 7. Comparison of thermal analysis results for the nuclear fuel pin and two proposed simulator designs (detailed in Fig. 2).

A small test fixture (Fig. 8) was fabricated to experimentally assess the performance of several thermal coupling materials that could be used in simulator buildup in attempt to match the effective fuel pin thermal conductivity and thermal diffusivity with an electrically heated simulator. The width of the container gap was selected to be 0.18 cm (0.070"), corresponding to the gap width in the Fig. 2c simulator design (shown with "powder or slurry" label). TCs are installed in grooves on the inner

and outer diameter of the vessel, with the measurement point at the axial midpoint of the heated region. A short high resistance heater element is installed at the center of the test fixture to indirectly heat the powder.

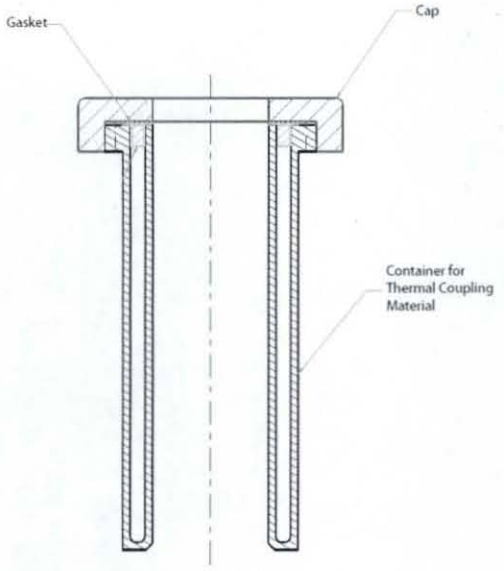

(a)

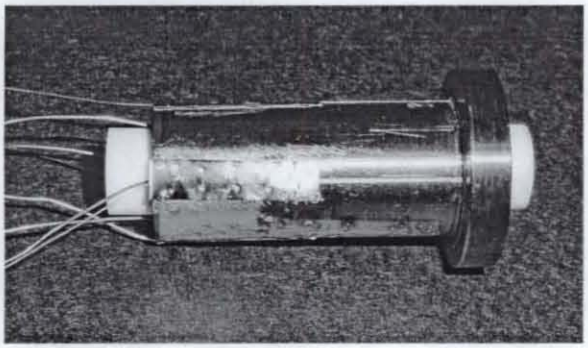

(b)

Fig. 8. Thermal coupling test vessel (a) engineering design and (b) hardware, prior to heater installation.

Materials considered in this initial testing include alumina (Al_2O_3), boron nitride (BN), aluminum nitride (AlN) and natural diamond powders. Properties are generally reported by vendors for the solid form of these materials, but thermal properties can be highly dependent on the packing fraction of a powder, and methods must be established fill the region to a specified density consistently each time a simulator is assembled. Theoretical fill material properties are reported in Bragg-Sitton et al.[10] Powder fill for initial tests is completed manually, with the aid of a metal "tamping" rod sized to fit the region; the fill material is further compacted by a metal gasket that is squeezed into place when the test fixture cap is screwed onto the filled container.

A series of tests indicate that packing fractions achieved for the tested powders range from 28% (Al_2O_3) to 53% (diamond) when compared to the theoretical material density, resulting in measured thermal conductivities that were approximately an order of magnitude less than predicted values. Temperature measurements made with an empty vessel indicated a *reduced* temperature drop relative to the powder filled gap. This result suggests a *higher* conductivity across the gap if it is only filled with helium gas and suggesting that the individual powder particles do not make good thermal contact with one another and, therefore, act more like a series of radiation shields that inhibit heat transfer across the gap. However, the inner and outer vessel walls were not thermally isolated, such that that there was no mechanism preventing heat flow along the container walls (Fig. 9). This could potentially cause an artificially high gap conductivity measurement if the heat transfer along the container walls (from the ID to the OD of the container) is significant relative to the heat transfer across the container gap. Subsequent testing of alternate fill materials will consider a redesigned test vessel in which the chamber walls are thermally isolated to further clarify the test results.

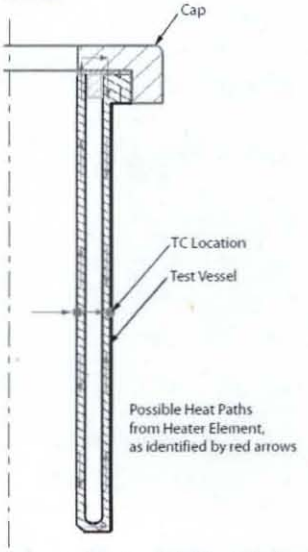

Fig. 9. Illustration of Potential Heat Paths from Heated TC in Interior Wall to TC on Outer Wall of Test Vessel.

Due to the relatively poor performance of the tested powder materials, an additional test was conducted for a carbonaceous cement slurry (UCAR Grade C-34, purchased from GrafTech, www.graftech.com). C-34 is composed of powder and liquid components that can be poured/injected into the test article gap using a small syringe. In this case, the density calculated from the fill volume and the mass of the test article before and after fill was approximately 94% of the predicted density. However, the thermal conductivity determined from temperature measurements across the cement filled contained was

approximately one quarter that of the vendor reported properties.

After completing tests at various power levels to obtain approximate properties over a range of temperatures, 3D x-ray analysis using computed tomography (CT) was conducted for the cement filled test article to further assess the uniformity of the filled region of the test container (minimum CT slice thickness and pixel resolution is 0.1092 mm). As shown in Fig. 10, the CT images qualitatively reveal that the cement density was not uniform in the gap, resulting in the marbling effect seen in the images. It is uncertain if the lower density regions resulted from a heterogeneous composition of the cement mixture (due to poor blending of the components) or from entrained air bubbles (resulting from manual mixing conducted in a glass beaker in room air). Entrained air bubbles could become voids when a vacuum environment is attained for testing, or could be filled with helium gas during test in the 600 torr helium environment that was selected for this application.

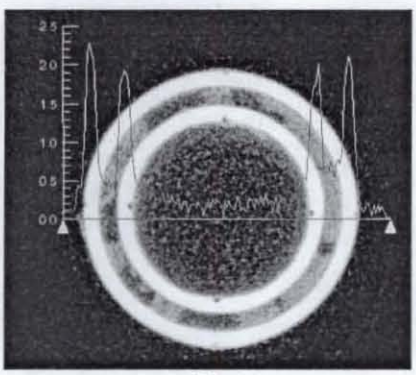

(a)

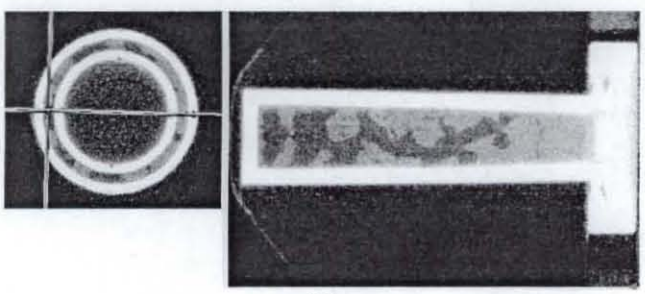

(b)

Fig. 10. CT results for the C-34 filled test article; (a) x-y cross section with qualitative plot of material density at the selected profile and (b) x-y and x-z images showing poor material distribution (crosshairs on x-y show selected plane for x-z image).

The calculated material packing fractions and measured temperature data acquired for the tested materials suggest that a slurry material, versus dry powder, can be used to more effectively and reliably fill a narrow gap in a simulator design, allowing one to attain properties much closer to theoretical values. However, CT analysis indicates the need to refine the mixing and fill techniques to provide uniform material composition and density in the filled region. Although thermal analysis indicates that the thermal diffusivity ($\alpha = k/\rho C_p$) of the tested cement is lower than desired to match the fuel element performance, a similar type of material (e.g. a conductive slurry) is being sought for the high fidelity simulator design study. A slurry hardens to become a permanent structure after it is baked in, but because it is contained between the insulator preform and the SS316 sheath it does not inhibit the ability to swap out the central heating element to study alternate power distributions. CT analysis will be used to develop a fill technique that produces uniformity in the filled region and reproducibility between test articles.

IV. CONCLUSIONS AND FUTURE HIGH FIDELTY SIMULATOR DEVELOPMENT

Fabrication of the initial advanced simulator hardware has demonstrated the ability to install instrumentation within the simulator structure without impinging on the simulator performance, while maintaining the option of heater element swap-out. However, the bottle shaped region of the simulator has proven to be difficult to fabricate for both the metal and ceramic components. Input from the individual component vendors is being sought to assist in refining and simplifying the design for the next stage in simulator development. Base element testing of the initial advanced simulator is now complete and testing with active heat removal in a water cooled calorimeter is set to commence, allowing testing to proceed at power levels typical of a fuel element in the baseline reactor design.

Advanced thermal simulator designs are currently being developed to further enhance the simulator performance relative to the predicted nuclear fuel pin performance. A variety of materials are currently being studied via thermal analysis to determine an optimal simulator design for transient performance matching, focusing on slurry materials to avoid the problems noted for powdered materials in the test results presented.

All initial testing has been conducted with constant diameter graphite heater elements. Graphite heating element designs with a modified cross section are now being refined to precisely match the approximate cosine-shaped axial power distribution observed for a nuclear fuel pin in the baseline reactor design, and it is anticipated that multiple heater designs will be tested in the simulator housing with active heat removal in the representative NaK flow cell. Although the central graphite heating element has been adopted for baseline simulator design, alternate heater designs are also being considered and, if available in sufficient time, could also be incorporated in the test plan for the current simulator design.

ACKNOWLEDGMENTS

The work described within this report was supported by NASA, in whole or part, as part of the agency's technology development and evaluation activities. Any opinions expressed are those of the author(s) and do not necessarily reflect the views of NASA.

NOMENCLATURE

T_{bulk}: bulk coolant temperature (K)
T_{max}: centerline temperature of fuel element or simulator (K)
q': liner heat rate (W/m)
k: thermal conductivity (W/m-K)
R: radius (Note: R_g is an average gap radius) (m)
h: convective heat transfer coefficient (W/m^2-K)
δ_l: fuel element liner thickness (m)
ρ: material density (kg/m^3)
C_p: specific heat capacity (J/kg-K)
α: thermal diffusivity (m^2/s)

Subscripts:
FE: fuel element
Sim: Simulator
f: fuel
l: liner
g: fuel gas gap
c: clad
s: sheath
x: simulator fill material
g1, g2: inner and outer simulator gas gaps
ci, co: clad, clad inner, clad outer
si, so: sheath, sheath inner, sheath outer

REFERENCES

1. V. CASAL, "Design of High-Performance Fuel Pin Simulators for Thermodynamic Experiments with Nuclear Fuel Elements," *Nuclear Technology*, **47**, 1, p. 153-162 (1980).

2. L.J. OTT and R. McCulloch, "Overview of Fuel Rod Simulator Usage at ORNL," in *Space Technologies and Applications International Forum (STAIF-2004)*, p. 703-712, edited by M.S. El-Genk, AIP Conf Proc 699, Melville, New York, 2004 (2004).

3. M. SURIANO, "TOPAZ-II Program: Initial US Demonstration Test Results on the TOPAZ-II Thermionic Space Nuclear Power System," in *Proceedings of the 28th Intersociety Energy Conversion Engineering Conference*, p. 855-861, American Chemical Society, Washington, D.C. (1993).

4. R.M. MASLO, "Hybrid Simulation of a Nuclear Fuel & Electric Heater Pin," in *Proceedings of the 8th AICA Congress*, p. 795-803, edited by L. Dekker, North-Holland Publishing Company, Amsterdam, Netherlands (1976).

5. S.M. BALASHOV, E.N. Videneev, A.V. Veresov, V.V. Zorichev, B.K. Mal'tsev, and V.N. Smolin, "Electrical Heaters for Experimental Installations and Nuclear Power Stations," *Thermal Engineering*, **49**, 5, p. 377-381 (2002).

6. S.M. BRAGG-SITTON and M. Forsbacka, "Application of a Virtual Reactivity Feedback Control Loop in Non-Nuclear Testing of a Fast Spectrum Reactor," in *proceedings of International Congress on Advanced Nuclear Power Plants (ICAPP-2004)*, p. 2259-2268, American Nuclear Society, La Grange Park, IL (2004).

7. T.J. GODFROY, R. Kapernick, and S.M. Bragg-Sitton, "Thermally Simulated 32kW Direct-Drive Gas-Cooled Reactor: Design, Assembly and Test," in *Proceedings of Space Technology and Applications International Forum (STAIF-2004)*, p. 757-763, edited by M.S. El-Genk, AIP Conference Proceedings 699, Melville, New York (2004).

8. M.K. VANDYKE, M.G. Houts, T.J. Godfroy, R. Dickens, J.J. Martin, D.I. Poston, P. Salvail and R. Carter, "Test Facilities in Support of High Power Electric Propulsion Systems," in *proceedings of Space Technology and Applications International Forum (STAIF-2003)*, p. 451-456, edited by M.S. El-Genk, AIP Conference Proceedings 654, Melville, New York, 2003 (2003).

9. M.K. VANDYKE, Martin, J.J., and Houts, M.G., "Overview of Nonnuclear Testing of the Safe, Affordable 30-kW Fission Engine Including End-to-End Demonstrator Testing," NASA/TM-2003-212930, NASA Marshall Space Flight Center, Huntsville, AL (2003).

10. S.M. BRAGG-SITTON, R. Dickens, D.D. Dixon, R. Kapernick, M. Adams and J. Davis, "Development of High Fidelity, Fuel-Like Thermal Simulators for Non-Nuclear Testing," in *Proceedings of Space Technology and Applications International Forum (STAIF-2007)*, p. 605-614, edited by M.S. El-Genk, AIP Conference Proceedings 880, Melville, New York (2007).

11. S.M. BRAGG-SITTON and Dickens, R., "Thermal Simulator Development: Non-Nuclear Testing of

Space Fission Systems," in *Transactions of the American Nuclear Society*, Vol. 95, p. 907-908, American Nuclear Society, La Grange Park, IL (2006).

12. J.A. ANGELO, and Buden, D., *Space Nuclear Power*, Orbit Book Company, Inc., Malabar, Florida, p.159-175 (1985).

13. R.S. FIELDER, D. Klemer and K. Stinson-Bagby, "High-Temperature Fiber Optic Sensors, an Enabling Technology for Nuclear Reactor Applications," in *Proceedings of the 2004 International Congress on Advances in Nuclear Power Plants*, Pittsburgh, PA, p. 2295-2305 (2004).

14. T.D. PANCZAK, S.G. Ring, M.J. Welch and D.A. Johnson, Thermal Desktop 5.0, Cullimore & Ring Technologies, Inc., Littleton, CO (2006).

15. B.A. CULLIMORE, S.G. Ring and D.A. Johnson, SINDA/FLUINT 5.0, Cullimore & Ring Technologies, Inc., Littleton, CO (2006).